JMB

Available online at www.sciencedirect.com

ScienceDirect

ELSEVIER

Hsp104 Targets Multiple Intermediates on the Amyloid Pathway and Suppresses the Seeding Capacity of Aβ Fibrils and Protofibrils

Muriel Arimon[1,2]†, Valerie Grimminger[1]†, Fausto Sanz[2] and Hilal A. Lashuel[1]*

[1]*Laboratory of Molecular Neurobiology and Neuroproteomics, Swiss Federal Institute of Technology Lausanne (EPFL), FSV-BMI AI 2137.1, Station 15, CH-1015 Lausanne, Switzerland*

[2]*Bioelectrochemistry and Nanotechnology Group, Department of Physical Chemistry, University of Barcelona, CIBER-BBN and IBEC, Baldiri Reixac 15, 08028 Barcelona, Spain*

The heat shock protein Hsp104 has been reported to possess the ability to modulate protein aggregation and toxicity and to "catalyze" the disaggregation and recovery of protein aggregates, including amyloid fibrils, in yeast, *Escherichia coli*, mammalian cell cultures, and animal models of Huntington's disease and Parkinson's disease. To provide mechanistic insight into the molecular mechanisms by which Hsp104 modulates aggregation and fibrillogenesis, the effect of Hsp104 on the fibrillogenesis of amyloid beta (Aβ) was investigated by characterizing its ability to interfere with oligomerization and fibrillogenesis of different species along the amyloid-formation pathway of Aβ. To probe the disaggregation activity of Hsp104, its ability to dissociate preformed protofibrillar and fibrillar aggregates of Aβ was assessed in the presence and in the absence of ATP. Our results show that Hsp104 inhibits the fibrillization of monomeric and protofibrillar forms of Aβ in a concentration-dependent but ATP-independent manner. Inhibition of Aβ fibrillization by Hsp104 is observable up to Hsp104/Aβ stoichiometric ratios of 1:1000, suggesting a preferential interaction of Hsp104 with aggregation intermediates (e.g., oligomers, protofibrils, small fibrils) on the pathway of Aβ amyloid formation. This hypothesis is consistent with our observations that Hsp104 (i) interacts with Aβ protofibrils, (ii) inhibits conversion of protofibrils into amyloid fibrils, (iii) arrests fibril elongation and reassembly, and (iv) abolishes the capacity of protofibrils and sonicated fibrils to seed the fibrillization of monomeric Aβ. Together, these findings suggest that the strong inhibition of Aβ fibrillization by Hsp104 is mediated by its ability to act at different stages and target multiple intermediates on the pathway to amyloid formation.

© 2008 Elsevier Ltd. All rights reserved.

Keywords: amyloid formation Aβ; Hsp104; disaggregation; Alzheimer's disease

Edited by S. Radford

Corresponding author. E-mail address: hilal.lashuel@epfl.ch.

† M.A. and V.G. contributed equally to this work.

Abbreviations used: Aβ₄₂, amyloid beta-(1–42); ATPγS, adenosine-5β-*O*-(3-thiotriphosphate); HD, Huntington's disease; Hsp, heat shock protein; Hsp104$_{TRAP}$, Hsp104 harboring the mutations E285Q/E687Q; Hsp104$_{WT}$, wild-type Hsp104; NBD, nucleotide-binding domain; PEP, phosphoenol pyruvate; PF, protofibril; PK, pyruvate kinase; SF, sonicated fibril; SEC, size-exclusion chromatography; TEM, transmission electron microscopy; ThT, thioflavin T; WT, wild type.

Introduction

Several neurodegenerative diseases are caused by protein misfolding and the accumulation of toxic aggregates in the cytoplasm (e.g., Lewy bodies in Parkinson's disease) or in the extracellular space (e.g., amyloid plaques in Alzheimer's disease) of neurons.[1] The ability of molecular chaperones to prevent protein misfolding and block or reverse protein aggregation-induced toxicity *in vitro* and *in vivo* has led to the hypothesis that some members of the chaperone system might play an active role in the disaggregation and clearance of amyloid fibrils *in vivo*. Molecular

chaperones function, either individually or in concert with other chaperones, to ensure the proper folding of newly synthesized polypeptides and the correct refolding of aggregation prone non-native states that would otherwise proceed to form amyloid fibrils. Amongst the different classes of molecular chaperones, only the yeast heat shock protein Hsp104 has been described to possess an amyloid–disaggregase activity, the ability to reverse fibril formation *in vitro*.[2,3] Hsp104 and its prokaryotic homologue ClpB are hexameric AAA+ ATPases with two nucleotide-binding domains (NBDs) per subunit that couple asymmetric cycles of ATP hydrolysis to the disaggregation of their polypeptide substrates. The substrate binding of ClpB/Hsp104 was shown to be dependent on the ATP state (Scheme 1a); accordingly, reduced or impaired ATP hydrolysis, as in the case of the

ATPase mutant E285Q/E687Q (Hsp104$_{TRAP}$), increases the affinity towards polypeptide substrates[5,7,8] (Scheme 1b). The processing of polypeptides by wild-type ClpB/Hsp104 results in the unfolding of non-native structures and separation of single polypeptides from aggregates, thus facilitating the refolding of proteins.[5,9,10] Several lines of evidence suggest that ClpB/Hsp104, in combination with the Hsp70/40 chaperone system, constitutes an efficient protein disaggregation machinery in bacteria, plants, and fungi, but not in metazoans.[4,11,12] In these organisms, ClpB/Hsp104 is directly involved in the disaggregation of stable protein aggregates after heat shock, and Hsp104 plays a central role in prion propagation of yeast cells.[13–15] Overexpression of Hsp104 reduces the aggregation and toxicity of mutant polyglutamine (polyQ) in animal models [polyQ is related to
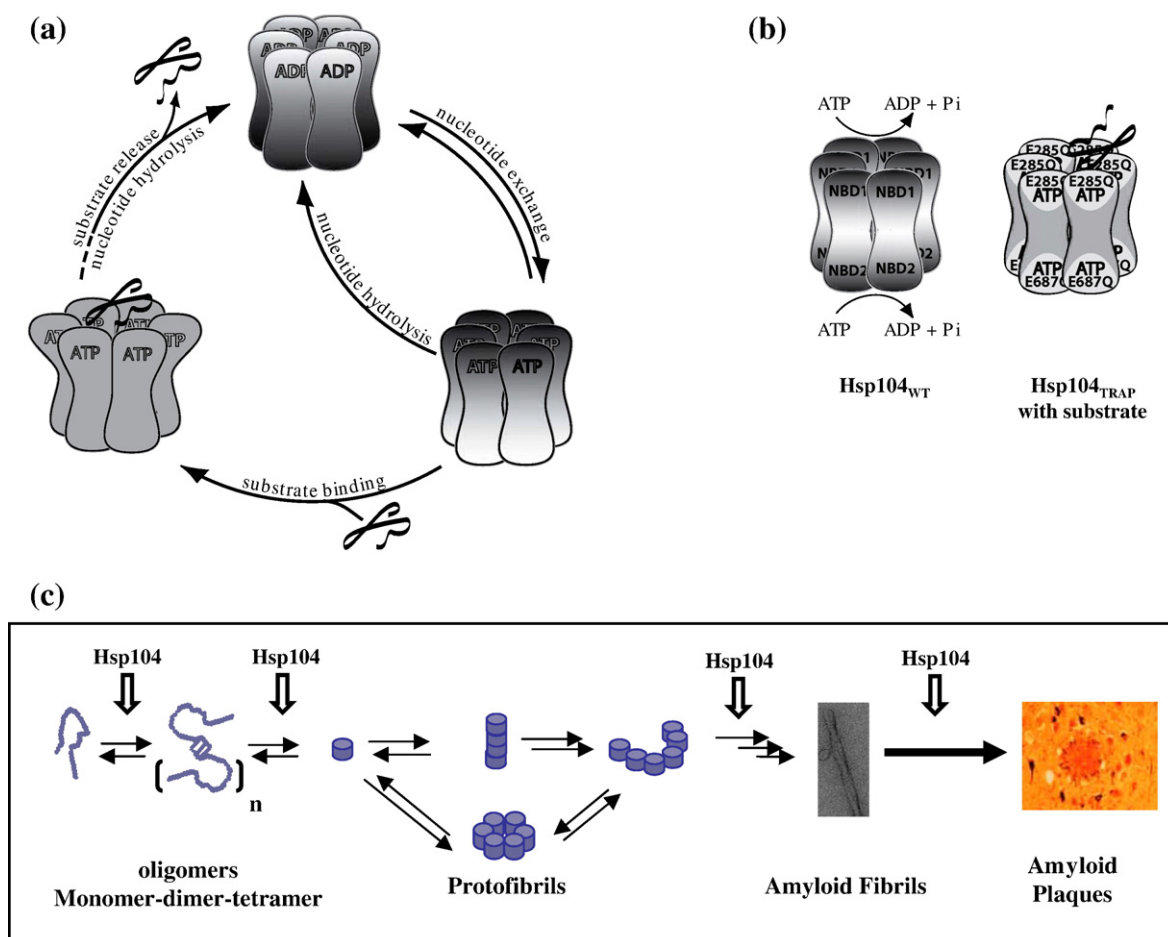
Scheme 1. High-affinity substrate binding by Hsp104 is dependent on its nucleotide state. (a) The ATPase-coupled substrate binding cycle of Hsp104$_{WT}$. During steady-state ATP hydrolysis, the NBD1 of Hsp104 cycles between different conformational states: an ADP-bound state with a low affinity towards polypeptide substrates and an ATP-bound state with a high affinity towards polypeptides. Accordingly, substrates bind to the ATP state, thereby generating a ternary Hsp104–ATP–substrate complex (left side). The ternary complex is committed to ATP hydrolysis. Adapted with modification from Ref. 4. (b) ATP turnover by Hsp104$_{WT}$ and Hsp104$_{TRAP}$. Hsp104$_{WT}$ cycles between different nucleotide states during steady-state ATP hydrolysis. However, tight substrate binding requires a (longer) ATP presence at NBD1. Thus, slowing down ATP hydrolysis improves substrate binding of Hsp104. No ATP hydrolysis takes place in the Trap mutant: the catalytic residues of Hsp104 are mutated; therefore, a permanent high-affinity state for substrate interaction is found when ATP is present.[5,6] (c) Hsp104 might interact with different species on the pathway of fibrillization and/or delay the aggregation of monomers, oligomers, protofibrils and fibrils of Aβ.
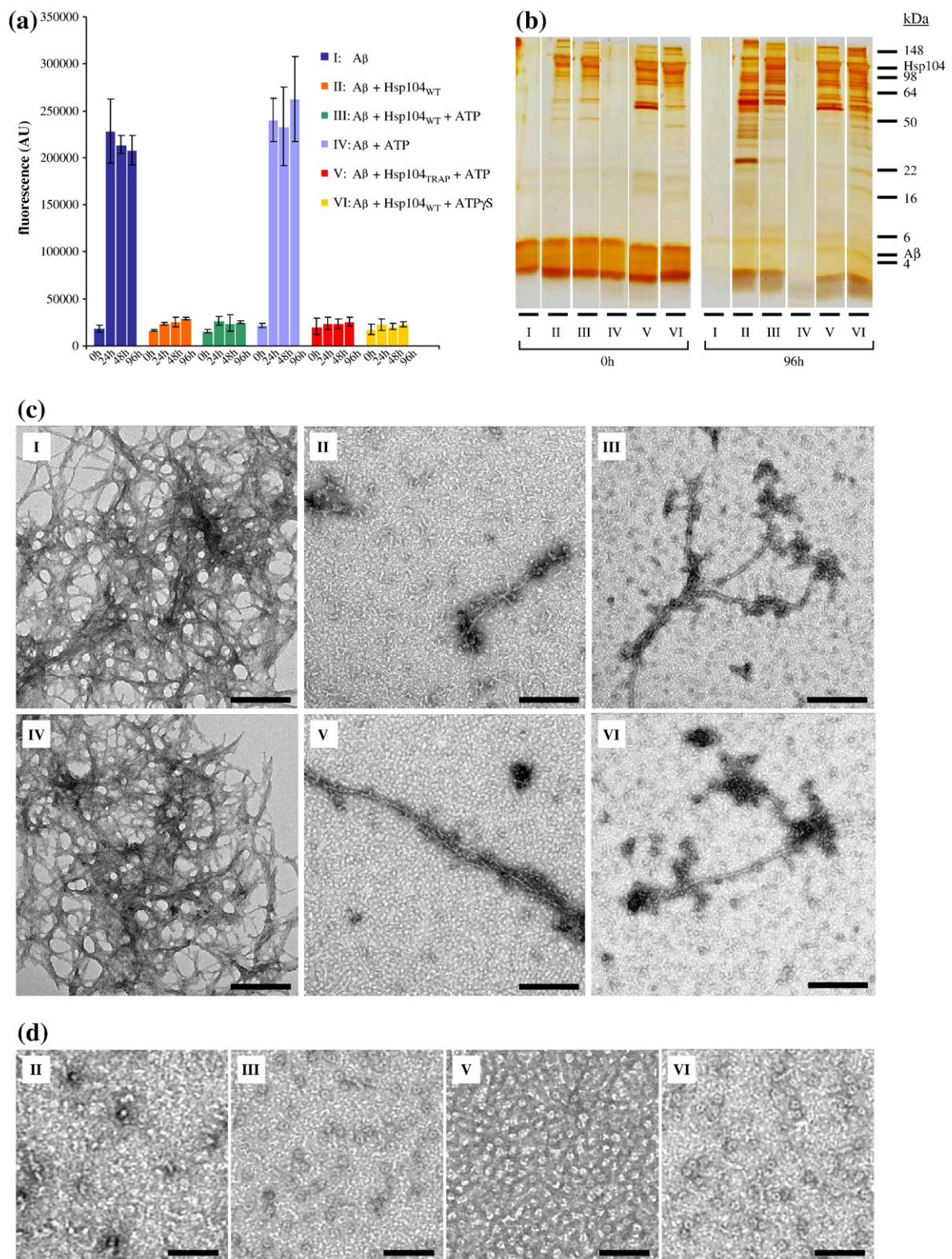
Fig. 1. Hsp104 prevents amyloid fibril formation of monomeric Aβ. (a) ThT fluorescence at different time points of aggregation of monomeric Aβ alone (I), Aβ with Hsp104$_{WT}$ (II), Aβ with Hsp104$_{WT}$ in the presence of ATP (III), Aβ only in the presence of ATP (IV), Aβ with Hsp104$_{TRAP}$ in the presence of ATP (V), and Aβ with Hsp104$_{WT}$ in the presence of ATPγS (VI). (b) SDS-PAGE analysis of the soluble fraction of the samples at the beginning (0 h) and at the end (96 h) of the experiment. The average fluorescence data from triplicate samples and standard deviation are plotted. (c) TEM images of the different samples at 96 h. The scale bar represents 200 nm. (d) Detailed view of the Hsp104 molecules in the samples at 96 h. The scale bar represents 40 nm.

Huntington's disease (HD)], mammalian cell cultures, and yeast models of HD.[16–20] Others have shown that Hsp104 alone can disassemble preformed Sup35 and Ure2 prion fibrils.[2,3] However, the molecular mechanisms underlying these effects remain poorly understood (Scheme 1c). It is noteworthy that in all the studies mentioned above it is not possible to discern whether the effects of Hsp104 are mediated by its unfoldase/disaggregase activity or simply through direct interactions with the monomeric or aggregated forms of the substrate.

The ability of Hsp104 to modulate the aggregation of different amyloid-forming proteins [e.g., polyQ, prion protein (PrP), Sup35, Ure2][3,20–23] suggests that it recognizes a common structural motif that is shared by the monomeric and/or aggregated forms of these proteins. To provide mechanistic insight into the molecular mechanism by which Hsp104 modulates protein aggregation and fibrillogenesis, we investigated the effect of Hsp104 on the oligomerization and fibril formation of the highly amyloidogenic peptide amyloid beta-(1–42) (Aβ$_{42}$) as a model substrate. Aβ peptide is the main constituent of amyloid plaques and plays a central role in the pathogenesis of Alzheimer's disease. Aβ$_{42}$ was chosen in particular because of its very well defined aggregation kinetics and the ease with which protofibrils and fibrils of Aβ$_{42}$ can be reproducibly prepared in high quantities.[24,25] Using an array of biophysical methods, we characterized the ability of Hsp104 to interact with the different intermediate species along the amyloid-formation pathway (Scheme 1c) and the consequences of these interactions on the fibrillization of Aβ. To probe the disaggregation activity of Hsp104, its ability to dissociate preformed aggregates of Aβ or block the seeding capacity of protofibrillar and

fibrillar Aβ was tested in the presence and in the absence of ATP (Scheme 1c). Together, our studies demonstrate that Hsp104 targets multiple intermediates on the amyloid pathway and suppresses the seeding capacity of Aβ fibrils and protofibrils. These studies shed new light on the molecular mechanisms by which Hsp104 modulates the aggregation and fibrillogenesis of amyloid-forming proteins in general.

Results

Hsp104 prevents amyloid fibril formation of monomeric Aβ

To probe the ability of Hsp104 to interfere with the aggregation of monomeric Aβ as well as the ATP dependency of this process, 10 μM of freshly isolated Aβ monomer was co-incubated with 1 μM of wild-type Hsp104 (Hsp104$_{WT}$) in the presence and absence of nucleotides. The aggregation process was monitored by thioflavin T (ThT) fluorescence, SDS-PAGE analysis, and transmission electron microscopy (TEM) at different time points. Aβ incubated alone showed a marked increase in ThT fluorescence within the first 24 h of incubation, after which the ThT values remained unchanged (Fig. 1a-I). When Hsp104$_{WT}$ was added to monomeric Aβ, the ThT values were similar to those of non-aggregated Aβ and remained unchanged during the course of the experiment (see 96 h in Fig. 1a-II), suggesting an Hsp104-mediated inhibition of Aβ fibrillization. Figure 1a-III shows that the presence of ATP did not enhance or reduce Hsp104-mediated inhibition of Aβ fibrillogenesis. The control sample with Aβ and ATP in the absence of Hsp104 (Fig. 1a-IV) exhibited
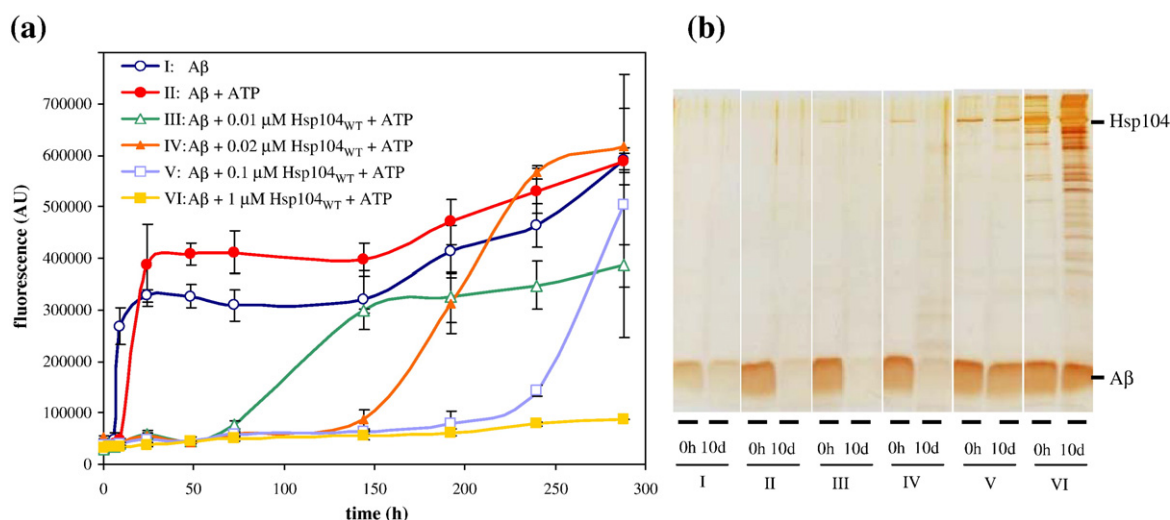

Fig. 2. Hsp104 hinders the aggregation of monomeric Aβ in a specific and concentration-dependent manner. (a) ThT fluorescence at different time points of the aggregation process of monomeric Aβ alone (I), Aβ with ATP (II), Aβ with 0.01 μM (III), 0.02 μM (IV), 0.1 μM (V), and 1 μM (VI) of Hsp104$_{WT}$ in the presence of ATP. The average fluorescence data from triplicate samples and standard deviations are plotted. (b) SDS-PAGE analysis of the soluble fraction of the samples at the beginning (0 h) and after 10 days of incubation. (c) TEM images of the samples at different time points.
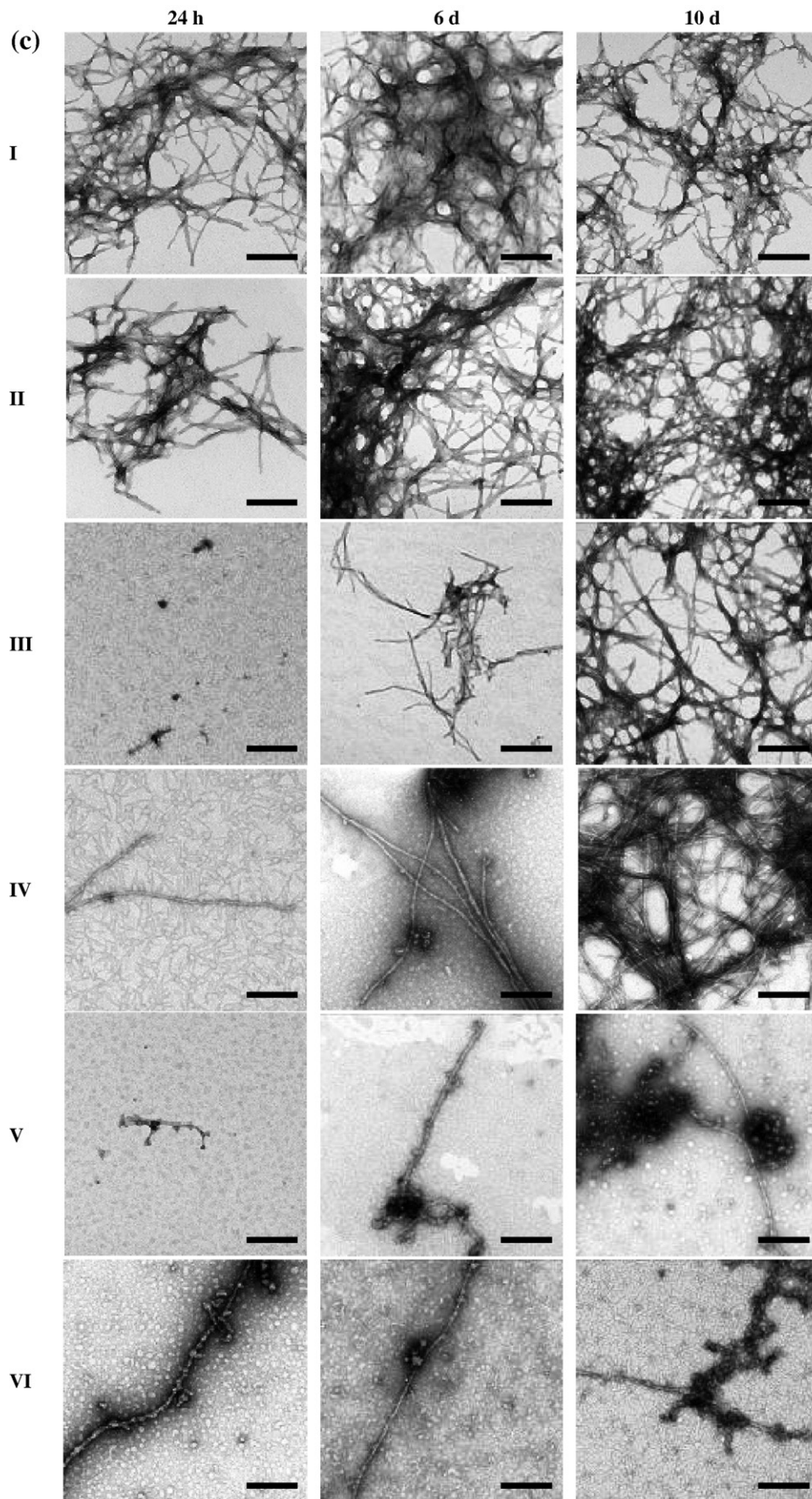
Fig. 2 (*legend on previous page*)

the same ThT pattern over time as the control sample containing only Aβ. To determine whether enhancing the interaction of Hsp104 with monomeric Aβ could increase its capacity to block Aβ oligomerization and fibrillogenesis, we artificially induced a high-affinity state of Hsp104 for the polypeptide by using two different strategies: (i) replacing the wild-type (Hsp104$_{WT}$) by the Trap mutant of Hsp104 (Hsp104-$_{TRAP}$) and (ii) adding adenosine-5β-O-(3-thiotriphosphate) (ATPγS). Hsp104$_{TRAP}$ contains two point mutations that render the chaperone unable to hydrolyze ATP (Scheme 1a and b).[4] On the other hand, ATPγS is an analogue of ATP that is hardly hydrolyzed by Hsp104.[5] In both cases, when Hsp104$_{TRAP}$ is used with ATP or Hsp104$_{WT}$ with ATPγS, the non-

hydrolyzed nucleotide remains bound to the chaperone, inducing a permanent high-affinity state for the substrate (Scheme 1a).[4] Aβ samples containing Hsp104$_{TRAP}$ in the presence of ATP as well as samples containing Hsp104$_{WT}$ with ATPγS did not show fibril formation, as demonstrated by the significant reduction in ThT values.

In order to quantify the remaining soluble protein (monomers, oligomers, and protofibrils), the samples were analyzed by SDS-PAGE. Aliquots of the different samples were centrifuged to remove insoluble material and the supernatant was subjected to gel electrophoresis. Figure 1b shows the level of soluble protein at the beginning (0 h) and at the end (96 h) of the aggregation procedure for each
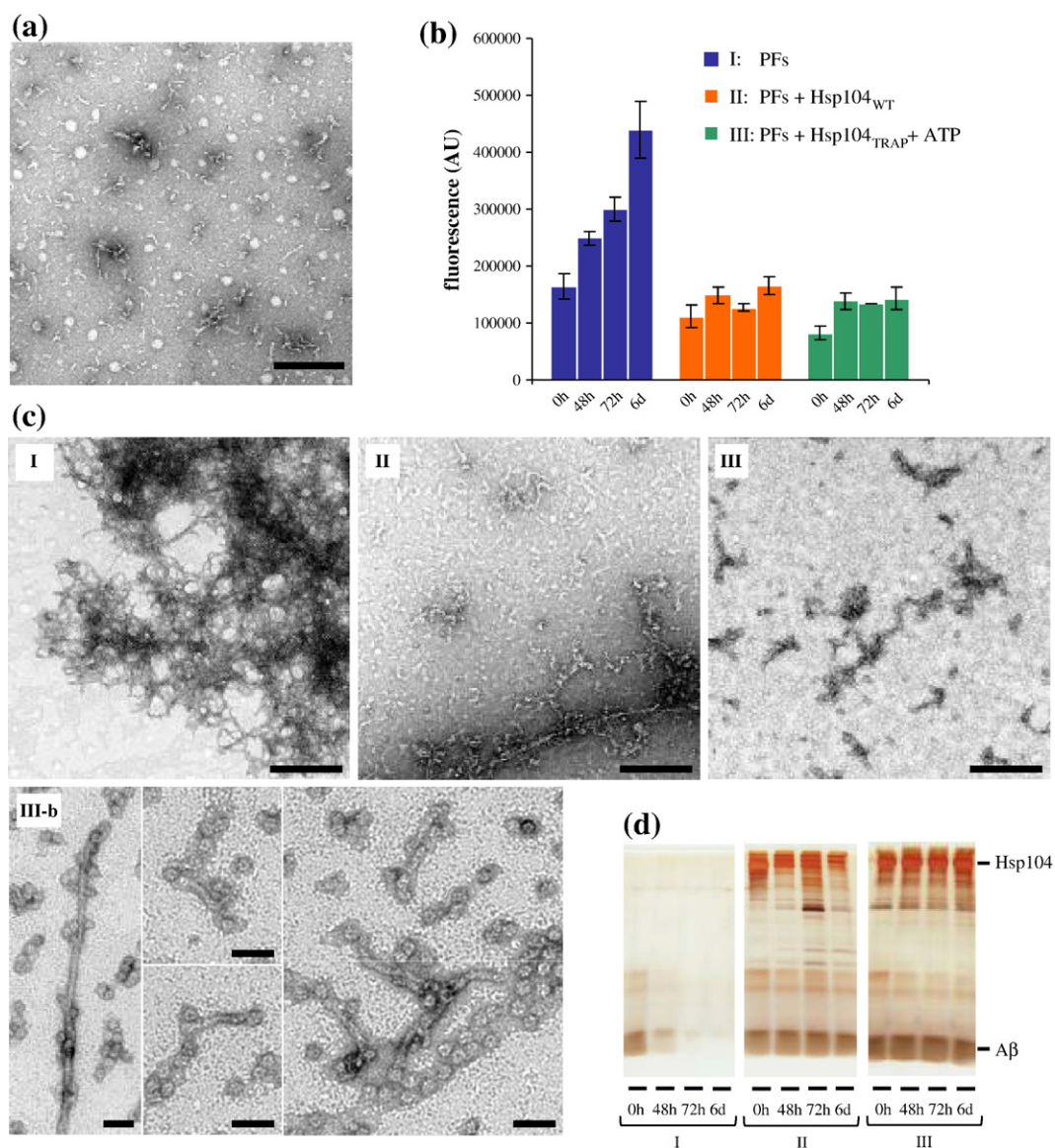

Fig. 3. Hsp104 prevents conversion of Aβ protofibrils into mature fibrils. (a) TEM image of freshly isolated protofibrils. The scale bar represents 200 nm. (b) ThT fluorescence at different time points of the aggregation process of protofibrils (PFs) alone (I), PFs with Hsp104$_{WT}$ (II), PFs with Hsp104$_{TRAP}$ in presence of ATP (III). The average fluorescence data from triplicate samples and standard deviation are plotted. (c) TEM images of the different samples at 72 h. The scale bar represents 200 nm. III in (b) shows the interaction of Hsp104$_{TRAP}$ with protofibrils in sample III. The scale bar represents 40 nm. (d) SDS-PAGE analysis of the soluble fraction of the samples at different time points.

sample. All samples containing Hsp104 showed that significant amounts of soluble Aβ (monomers and protofibrils) remain in the supernatant after 96 h of incubation. In contrast, samples containing Aβ alone or Aβ with ATP did not show any band corresponding to Aβ after 96 h of incubation at 37 °C, suggesting that almost all soluble Aβ has been converted into insoluble fibrils under these conditions. The reduced intensity of the Aβ bands at 96 h is due to staining artifact in this specific case and does not reflect reduced levels of soluble Aβ (see Figs. 2, 3, and 4). In agreement with the ThT data, the TEM images at 96 h showed dense networks of fibrils in samples of Aβ alone or Aβ with ATP (Fig. 1c-I and -IV). In contrast, samples containing Hsp104 did not show mature fibrils but rather some Aβ oligomers and protofibrils (Fig. 1c-II, -III, -V, and -VI). This observation was not dependent on the Hsp104 variant or the presence/absence of nucleotide. In the samples containing ATP, we observed predominantly spherical, ring-like structures, which presumably correspond to hexameric Hsp104 molecules (Fig. 1c-II, -III, -V, -VI,

and d). When Hsp104 was incubated in the absence of Aβ, we did not observe any aggregation or fibril formation (see Hsp104 alone in Supplementary Fig. S1). In summary, Hsp104 blocks the fibrillization, but not the oligomerization, of Aβ. The inhibitory effect of Hsp104 is independent of the presence of nucleotides or of the nucleotide-binding capacity of Hsp104.

Hsp104 inhibits the fibrillization of monomeric Aβ in a specific and concentration-dependent manner

In order to evaluate the effect of Hsp104 concentration on Aβ, the kinetics of Aβ aggregation was analyzed in the presence of ATP at different Hsp104 concentrations. Since we did not observe any fibril formation at an Hsp104 concentration of 1 μM (at least up to 96 h of incubation), lower concentrations of Hsp104$_{WT}$ were explored (Fig. 2). The control sample containing only Aβ showed the characteristic sigmoid ThT fluorescence curve (Fig. 2a-I) with a lag phase (0–9 h) followed by a rapid increase in
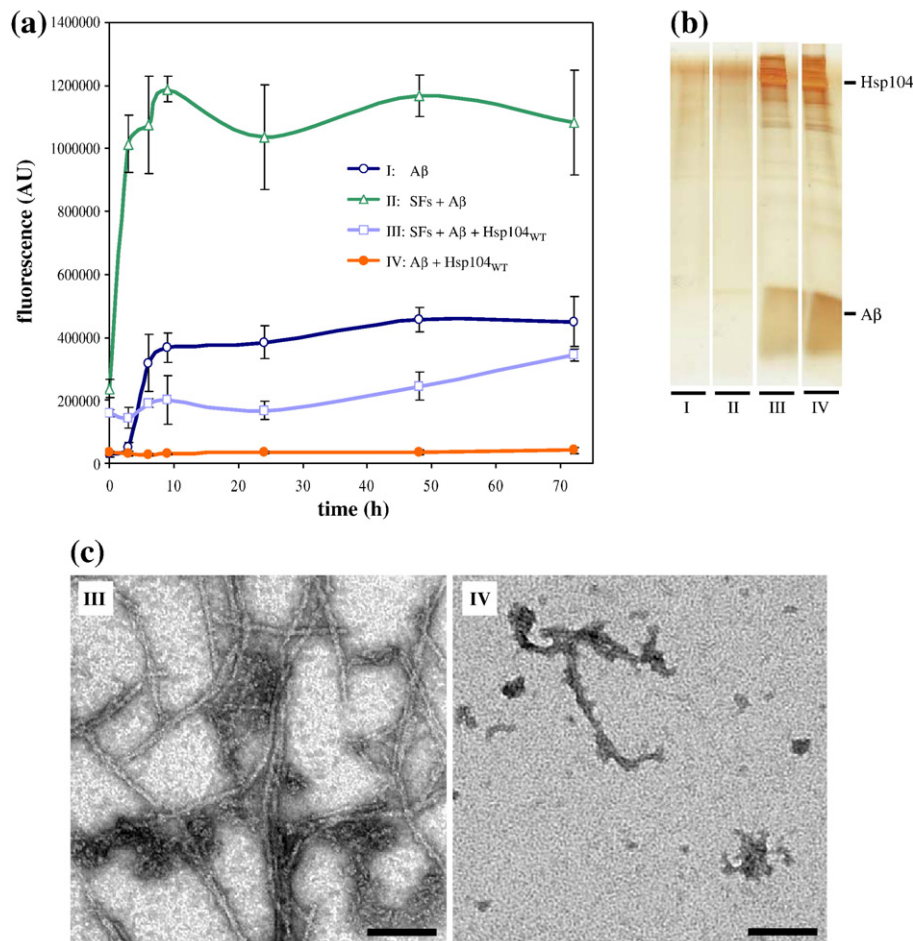

Fig. 4. Hsp104 abolishes the seeding capacity of fibrillar Aβ. (a) ThT fluorescence at different time points of the aggregation process of Aβ monomer alone (I), Aβ monomer seeded with 2.2 μM SFs (II), Aβ monomer seeded with 2.2 μM SFs in the presence of Hsp104$_{WT}$ (III), and monomeric Aβ in the presence of Hsp104$_{WT}$ (IV). The average fluorescence data from triplicate samples and standard deviation are plotted. (b) SDS-PAGE analysis of the soluble fraction of the samples at 72 h. (c) TEM images of samples III and IV at 72 h. The scale bars represents 100 nm.

the ThT signal (9–24 h) before a plateau was reached. Similar aggregation kinetics were observed in the presence of ATP (Fig. 2a-II). A concentration-dependent delay of Aβ aggregation was found in the range of 0.01 to 1 μM Hsp104. In the presence of 0.01 μM Hsp104, a significant delay in the lag phase was observed when compared to the control, i.e., the ThT fluorescence started to rise after 72 h (Fig. 2a-III) instead of a lag time of 9 h for the control sample. When the Hsp104 concentration was increased to 0.02 μM, the lag phase extended to ~6 days (144 h, Fig. 2a-IV). This delay was increased to ~8 and >12 days at Hsp104 concentrations of 0.1 (Fig. 2a-V) and 1 μM (Fig. 2a-VI), consistent with a concentration-dependent inhibition of Aβ fibrillization by Hsp104. Figure 2b shows the SDS-PAGE analysis of Aβ samples in the presence of increasing concentrations of Hsp104 at the beginning and after 10 days of aggregation. After incubation for 10 days, samples containing monomeric Aβ alone, Aβ with ATP, or Aβ with either 0.01 or 0.02 μM Hsp104 showed almost no Aβ monomer in the supernatant fraction. Samples with higher amounts of Hsp104, 0.1 and 1 μM, showed a band of Aβ of the same intensity as in the time-zero lanes, consistent with the ThT results. TEM images of the samples at different time points are shown in Fig. 2c. Samples without Hsp104, such as Aβ alone or Aβ with ATP, showed predominant bundles of mature fibrils already after 24 h (Fig. 2c-I, -II). However, samples containing Hsp104, regardless of their concentration, showed almost no fibrillar structures but small and amorphous aggregates (Fig. 2c-III to -VI). After 6 days of incubation, the sample with the lowest concentration of Hsp104 (0.01 μM) contained some disperse bundles of mature fibrils (Fig. 2c-III), while the sample with 0.02 μM Hsp104 showed quite long but isolated fibrils (Fig. 2c-IV). At concentrations of 0.1 or 1 μM Hsp104 (Fig. 2c-V, -VI), very few fibrils were observed. After 10 days of incubation, all samples showed the presence of dense networks of fibrils, except for those containing 0.1 or 1 μM Hsp104. Samples containing 0.1 μM Hsp104 showed some long dispersed fibrils (Fig. 2c-V) and in the sample containing 1 μM Hsp104 very few fibrillar species were observed (Fig. 2c-VI).

Hsp104 prevents conversion of Aβ protofibrils into fibrils

Protofibrils are intermediate species that precede amyloid fibril formation in the aggregation pathway of Aβ.[26–28] The term protofibrils refers to a complex mixture of species of heterogeneous size and morphology, including spheres, pore-like structures, and chain-like species.[24] Protofibrils are on-pathway intermediates and convert into mature amyloid fibrils.[26,29–31] To probe the ability of Hsp104 to interact with these structures and to determine the consequences of such interactions on the stability and fibrillization of protofibrils, freshly isolated protofibrils (Fig. 3a) were co-incubated with Hsp104 and the aggregation was monitored by

ThT fluorescence, TEM, and SDS-PAGE. Upon incubation at 37 °C, the sample containing protofibrils alone showed a gradual increase in ThT signal with time (Fig. 3b-I), consistent with a conversion of the protofibrils into mature fibrils. However, co-incubation of the same structures with Hsp104_WT inhibited fibrillization even after 6 days of incubation (Fig. 3b-II). A similar effect was observed when protofibrils were incubated with Hsp104_TRAP together with ATP (Fig. 3b-III). In all cases, no change in ThT signal was observed, suggesting that a dissociation of the protofibrils did not take place, at least not under the experimental conditions that were used here. Consistent with this hypothesis, TEM analysis of the samples containing either Hsp104_WT or Hsp104_TRAP showed only some isolated short fibrils but mainly protofibrillar structures similar to those present at the starting conditions (Fig. 3c-II, -III). As expected, samples containing protofibrils alone showed dense networks of fibrils after 72 h of incubation (Fig. 3c-I). Interestingly, in the sample containing the TRAP mutant, some ringlike structures, most likely Hsp104 molecules, were found to be interacting with the protofibrils (Fig. 3c-III-b, see also Fig. 1d-V). This could be due to the stabilized hexamerization state and increased affinity of the Hsp104_TRAP for the substrate.[4] To confirm the ThT and TEM results, an SDS-PAGE analysis was performed to quantify the remaining amount of soluble Aβ species (monomers, oligomers, and protofibrils) at different time points (Fig. 3d). Aβ protofibrils generated with our protocol are SDS sensitive and run as a band corresponding to monomeric Aβ. In the absence of Hsp104, a significant decrease in the amount of soluble Aβ was observed over time. However, protofibril samples containing either Hsp104_WT or Hsp104_TRAP showed no change in the Aβ band intensity throughout the experiment, in agreement with the ThT and TEM data.

Hsp104 abolishes the seeding capacity of fibrillar Aβ

To further characterize the possible interaction of Hsp104 with the small aggregates or nuclei on the amyloid pathway of Aβ, the ability of Hsp104 to enhance or inhibit the seeding capacity of Aβ fibrils was investigated. It is well established that the addition of aggregation nuclei (preformed fibril "seeds") at the beginning of the process accelerates fibril formation and abolishes the characteristic lag phase.[32,33] To create effective Aβ seeds, mature Aβ fibrils were mechanically disrupted by sonication to yield a narrow distribution of short fibrils, hereinafter referred to as sonicated fibrils (SFs). These seeds did not reassociate to mature fibrils at low concentrations (2.2 μM) within the time frame of the experiments (Supplementary Fig. S2). Monomeric Aβ fibrillization showed the typical sigmoid ThT fluorescence curve (Fig. 4a-I). As expected, addition of small amounts of fibrillar seeds (SFs) abolished the lag phase and accelerated Aβ fibrillization (Fig.

4a-II); notably, due to the ThT binding of SF, the ThT baseline signal at $t = 0$ h was slightly higher in the samples in Fig. 4a-II and -III. Interestingly, addition of Hsp104$_{WT}$ to the mixture of monomeric Aβ with SFs abolished the seeding effect (Fig. 4a-III). TEM images of the samples at 72 h displayed dense networks of short fibrils when no Hsp104 was present, whereas the seeded Aβ sample with Hsp104$_{WT}$ showed predominantly spherical structures (Fig. 4c-III). When Hsp104 was added to the sample containing only Aβ monomer, no fibril formation was observed (Fig. 4c-IV). Moreover, when Hsp104 was added to the SFs alone, without Aβ monomer, no decrease in the ThT signal was observed within the duration of the experiment (Supplementary Fig. S2), ruling out any disaggregation of these structures by Hsp104. SDS-PAGE analysis of these samples after 72 h incubation (Fig. 4b) revealed that some soluble forms of Aβ (monomers and proteofibrils) persist in the samples containing Hsp104, whereas no soluble Aβ could be detected in the supernatant of samples lacking Hsp104 (Fig. 4b-III and -IV), which is in good agreement with the ThT data. These results suggest that Hsp104 abolishes the seeding capacity of fibrillar Aβ.

Hsp104 abolishes the seeding by Aβ protofibrils

Protofibrils can also be used to seed the aggregation of Aβ.[25] To probe the effect of Hsp104 on the

seeding ability of Aβ protofibrils, a seeded aggregation assay with 10 μM protofibrils was carried out in the presence and in the absence of Hsp104. When monomeric Aβ was incubated for 96 h with 10 μM protofibrils, the ThT signal reached values that were approximately two times higher than those observed for Aβ protofibrils alone and the lag phase was significantly shortened (Fig. 5a-II *versus* a-I). Co-incubation of Aβ monomer and protofibrils with Hsp104 significantly reduced their seeding capacity (Fig. 5a-III). Figure 5b shows that addition of Hsp104 to a mixture of monomeric Aβ and protofibrils resulted in the accumulation of predominantly protofibrillar aggregates and some short flexible fibrillar structures (Fig. 5b-III). These structures differed significantly from the corresponding sample lacking Hsp104 (Fig. 5b-II) and suggest that Hsp104 also abolishes the seeding ability of protofibrillar Aβ, possibly via direct interactions with either Aβ protofibrils or monomers or both.

Hsp104 prevents further association of mature Aβ fibrils

Hsp104 has been reported to possess the unique ability of disrupting and resolubilizing stable protein aggregates.[2,3] To probe the ability of Hsp104 to disaggregate amyloid fibrils, Hsp104$_{WT}$ was incubated with preformed mature Aβ fibrils. Since Aβ has a strong propensity to form highly compact networks of fibrils (Fig. 1c-I), which could reduce
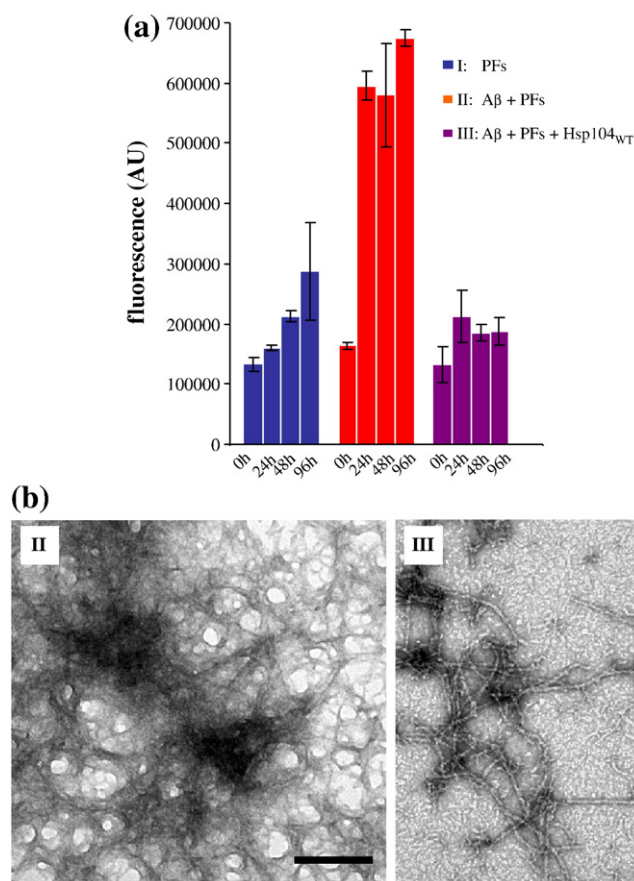

Fig. 5. Hsp104 abolishes the seeding of monomeric Aβ by protofibrils. (a) ThT fluorescence at different time points of the aggregation process of PFs alone (I), Aβ monomer seeded with PFs (II), and Aβ monomer seeded with PFs in the presence of Hsp104$_{WT}$ (III). The average fluorescence data from triplicate samples and standard deviation are plotted. (b) TEM images of samples II and III at 24 h.

the accessibility to Hsp104, Aβ fibrils were sonicated to generate short fibrils with a narrow size distribution (Fig. 6c). The SFs were incubated in the presence and in the absence of Hsp104$_{WT}$ and ATP. To ensure the continuous supply of ATP throughout the incubation process, an ATP-regenerating system composed of pyruvate kinase (PK) and phospho-*enol*pyruvate (PEP) was included. The sample containing SFs with Hsp104 and ATP/PK/PEP showed a low ThT fluorescence that remained unchanged during the experiment (Fig. 6a-II). This ThT signal was lower than the signal of the control sample lacking Hsp104 and ATP/PK/PEP at the start of the experiment. To check whether this difference in ThT fluorescence at $t = 0$ h was due to an initial Hsp104-induced dissociation of pre-formed fibrils or due to interference with ThT fluorescence by the ATP-regenerating system, SFs were incubated with ATP/PK/PEP in the absence of Hsp104 (Fig. 6a-III). The addition of the ATP-regenerating system to SFs also resulted in an initial decrease in the ThT signal, suggesting an interference with the ThT fluorescence. Although this sample showed significantly lower ThT values

compared to the controls with only SFs, a continuous increase in the ThT signal was observed over time, suggesting that the presence of the ATP-regenerating system does not interfere with the reassociation of mature fibrils. To check for any disaggregation of the mature fibrils by Hsp104, we determined the amount of soluble Aβ in the samples at the end of the experiment by centrifugation and SDS-PAGE analysis of the supernatant (Fig. 6b). In all samples, no soluble Aβ was detected, suggesting that Hsp104 does not induce the dissociation of preformed fibrils into monomers or other soluble species. To verify these findings, all samples were examined using TEM. The starting SF material showed short and evenly distributed fibrils throughout the grid (Fig. 6c). After 96 h, the samples containing SFs alone, or SFs in the presence of ATP/PK/PEP but without Hsp104, exhibited large networks of fibrils (Fig. 6d-I and -III). Interestingly, SFs incubated in the presence of Hsp104$_{WT}$ and ATP/PK/PEP were lacking mature fibrils but contained predominantly short fibrils decorated with spherical structures, presumably Hsp104 hexamers (Fig. 6d-II).
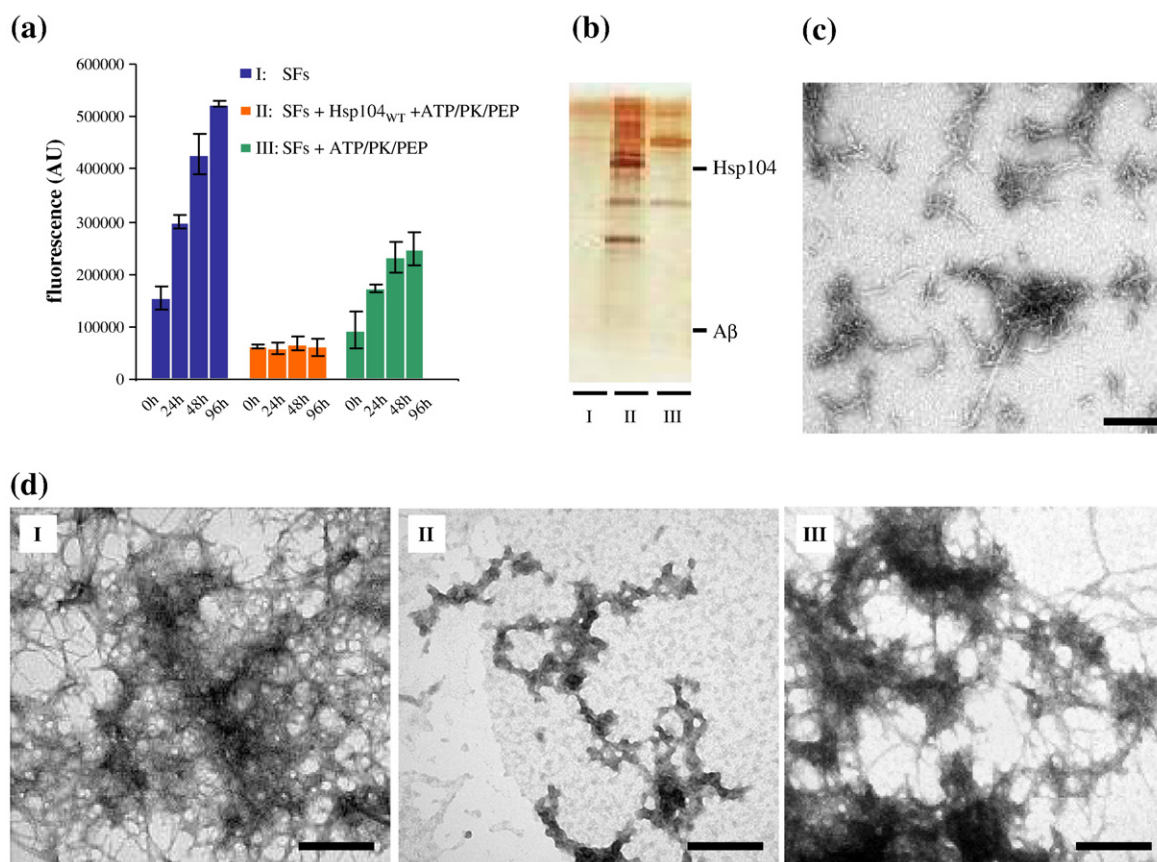

Fig. 6. Hsp104 prevents further aggregation of mature Aβ fibrils. (a) ThT fluorescence at different time points of the aggregation process of 10 μM sonicated mature fibrils (SFs) alone (I), 10 μM SFs with Hsp104$_{WT}$ in the presence of ATP/ PK/PEP (II), and 10 μM SFs only in the presence of ATP/PK/PEP (III). The average fluorescence data from triplicate samples and standard deviations are plotted. (b) SDS-PAGE analysis of the soluble fraction of the different samples at the end of the experiment. (c) TEM image of the starting preparation of SFs. The scale bar represents 100 nm. (d) TEM images of the different samples at 96 h. The scale bars represents 200 nm.

Hsp104 inhibits Aβ aggregation at different stages of the fibrillization process

Thus far, the current results using purified Aβ monomers and different aggregation states suggest that Hsp104 interferes with Aβ fibrillization by interacting with different aggregation intermediates along the amyloid-formation pathway. It blocks the fibrillization of monomeric and protofibrillar Aβ as well as the reassociation and growth of fibrillar Aβ.

To confirm these findings, the aggregation of monomeric Aβ was followed and the effect of introducing Hsp104 at different time points during the fibrillization process was probed. When Hsp104 was present from the very beginning of the experiment (Fig. 7a-II) or added 4 h after the start of the incubation of monomeric Aβ (Fig. 7a-III), no fibril formation was observed by ThT and TEM during the course of the experiment. Addition of Hsp104 at later time points (6 and 9 h) resulted in an immediate inhibition of
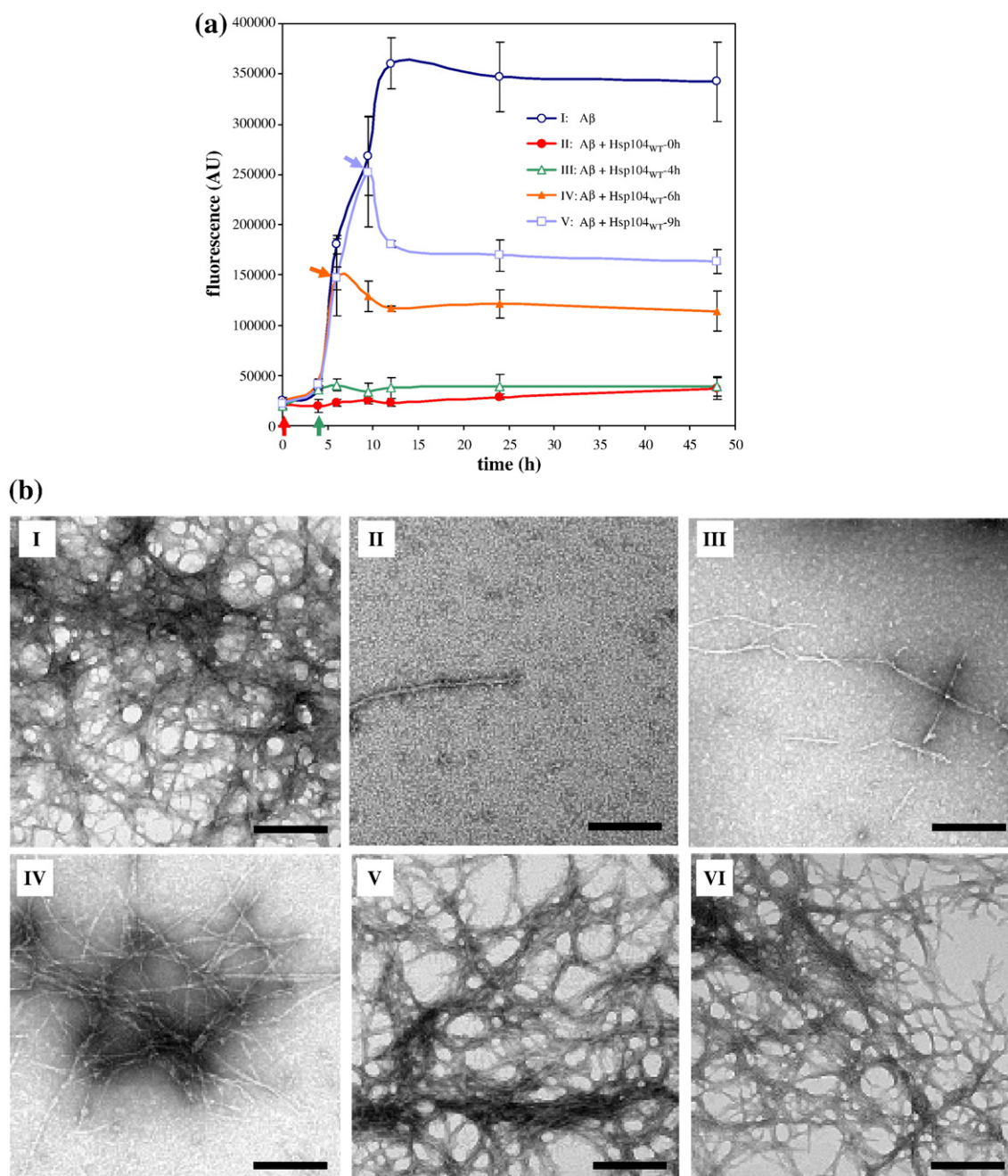

Fig. 7. Hsp104 hinders Aβ aggregation at different stages of the aggregation process. (a) ThT fluorescence at different time points of the aggregation process of monomeric Aβ alone (I), monomeric Aβ with Hsp104$_{WT}$ added at the beginning of the experiment (II) or after 4 h (III), 6 h (IV) and 9 h (V). The average fluorescence data from triplicate samples and standard deviations are plotted. (b) TEM images of the same samples after 9 h of aggregation.

amyloid formation as discerned by the stabilization of the ThT signal upon addition of Hsp104 (Fig. 7a-IV and -V). In the latter cases, a sudden decrease in ThT was consistently observed, but no further decline in the ThT signal occurred even after the Aβ-Hsp104 mixture was incubated for an additional period of 40 h. The sudden decline in ThT signal could be attributed to the strong binding of Hsp104 to Aβ aggregates and competition for ThT binding sites. These findings are consistent with the results obtained with purified protofibrillar and fibrillar Aβ species (also visible in Supplementary Fig. S2) and support the notion that Hsp104 interacts preferentially with aggregated forms of Aβ, including protofibrils and fibrils, but does not promote transitions from protofibrils or fibrils to monomers. The fibrillization state, which stays "frozen" by the addition of Hsp104, was monitored by TEM. Figure 7b demonstrates that the actual state of fibrillization corresponds well to the different levels of ThT fluorescence in the samples.

Binding of Aβ can be monitored by ATP turnover of Hsp104 and by size-exclusion chromatography co-elution

The aggregation assays shown above demonstrate that ATP is not required for the inhibition of Aβ aggregation by Hsp104, indicating a novel nucleotide-independent interaction mechanism of Hsp104. However, previous studies suggested that Hsp104–substrate interaction is highly dependent on its nucleotide state.[4] Furthermore, substrate binding in turn also influences the ATP turnover by Hsp104.[5] Consequently, the ATPase activity of Hsp104 can be used as an indirect measure of substrate binding. Accordingly, the ATP consumption by Hsp104 in the presence of different con-

centrations of monomeric and protofibrillar Aβ was measured using a regenerative ATPase assay system.[34] Figure 8 shows that the addition Aβ to Hsp104$_{WT}$ enhanced its ATPase activity in a concentration-dependent manner. Monomeric Aβ accelerated the ATPase activity of Hsp104 by a factor of ~2, whereas protofibrillar Aβ showed a rather weak effect. The ATPase data suggest a direct interaction between the two proteins and the recognition of Aβ by Hsp104 as its substrate. These findings are in good agreement with other studies that show an acceleration of the Hsp104 ATPase activity upon binding of substrates such as permanently unfolded RCMLA (reduced carboxymethylated α-lactalbumin).[5,35] However, one study by Schirmer and Lindquist showed a weak inhibition by Aβ$_{42}$ with a reduction by a factor of 0.8.[23] This discrepancy might be due to differences in the aggregation state of Aβ or assay conditions such as salt content, pH, the presence of traces of denaturants (guanidinium chloride), and peptide concentration, to which Hsp104 is highly sensitive.[6,34]

Beyond the ATPase assays, which are an indirect measure of the substrate interaction, direct methods were employed to study the binding of Aβ to Hsp104. Size-exclusion chromatography (SEC)–HPLC co-elution experiments were performed on samples of Hsp104 in the presence and in the absence of monomeric and protofibrillar Aβ. The eluted fractions from the SEC column were analyzed by a dot blot using antibodies against Aβ and Hsp104, respectively (Fig. 9). In the first experiment, a co-elution of Aβ monomer with the high molecular weight species (corresponding to Hsp104) was indicative of the interactions between Hsp104 and Aβ. The dot blot shows that the Aβ monomer co-eluted with Hsp104 in earlier fractions than the sample containing Aβ monomer alone (Fig. 9a). When Hsp104 was incubated with Aβ protofibrils and injected into the column, the dot blot reveals that a proportion of Hsp104 eluted earlier together with the protofibrillar fractions. Consequently, Hsp104 interacts with both monomeric and protofibrillar forms of Aβ. However, it is important to note that these experiments provide a qualitative rather than a quantitative measure of the binding of Hsp104 to Aβ. Interestingly, in both types of experiments, binding of Hsp104 to Aβ monomer and protofibrils, the addition of ATP, ADP, or ATPγS did not influence the co-elution profile (data not shown). This nucleotide-independent interaction between Hsp104 and Aβ is in good agreement with the results of the fibrillization assays described above. The current co-elution experiment did not show a complete binding of Aβ to Hsp104 but rather a co-elution of a minor fraction of Aβ molecules with Hsp104 (and *vice versa* for protofibrils), indicating a transient substrate interaction. These results differ from previous findings where co-elution of Hsp104 with its substrates (RCMLA, TrfA, α-casein, aggregated glucose-6-phosphate dehydrogenase, and β-galactosidase-derived peptides) was suggested to be strictly dependent on the presence of non-
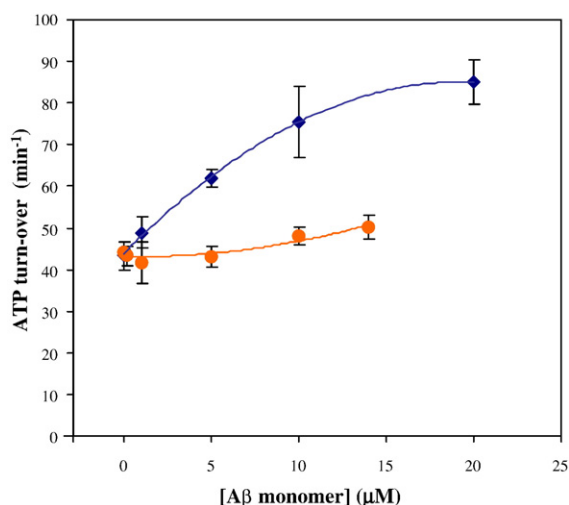

Fig. 8. Influence of Aβ monomer on the ATP turnover of Hsp104$_{WT}$. ATP turnover of 0.2 μM Hsp104 determined in the presence of increasing concentrations of Aβ monomer (♦) or Aβ protofibrils (●).
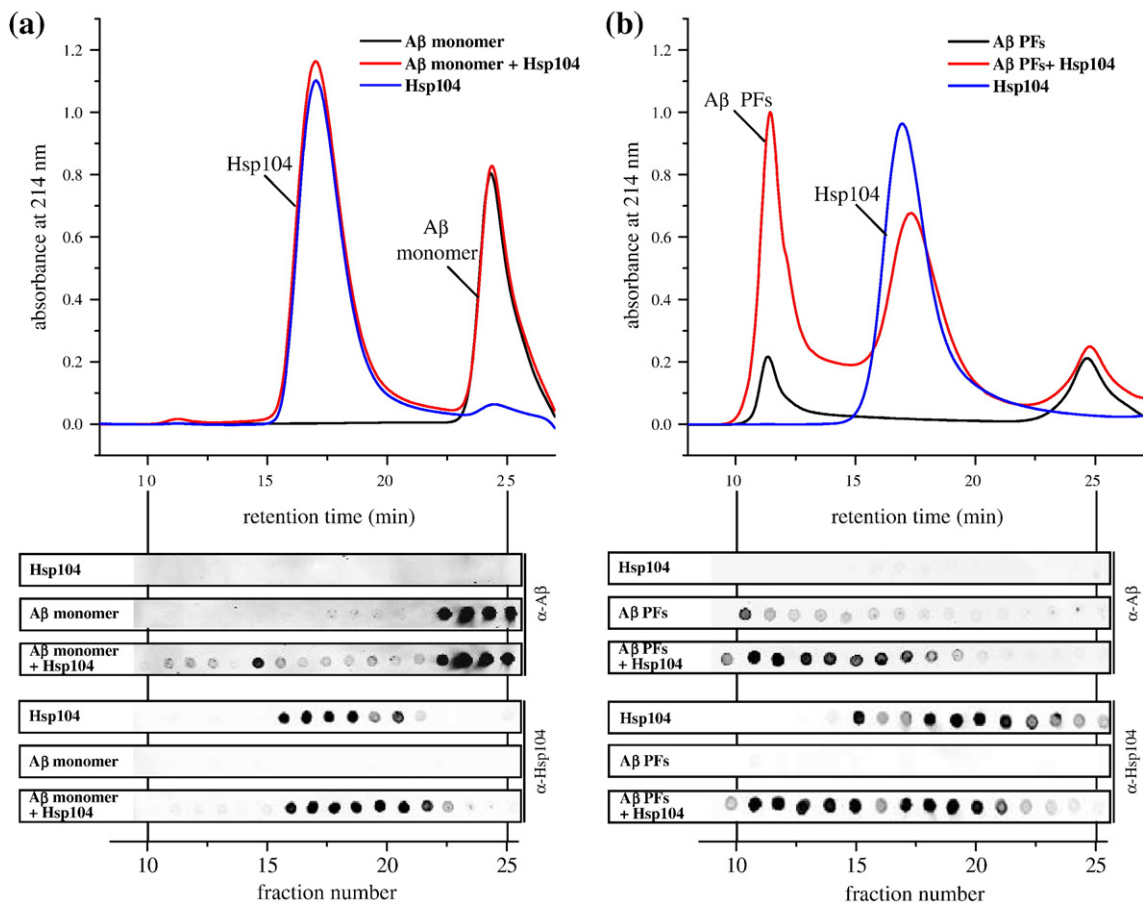
Fig. 9. Co-elution analysis of Hsp104$_{WT}$ with Aβ monomer (a), or Aβ protofibrils (b). Hsp104 (5 μM) was incubated with (a) freshly prepared Aβ monomer (40 μM) or (b) Aβ PFs (100 μM) at room temperature for 30 min. Subsequently, the samples were subjected to SEC–HPLC using a Superose 6 column. Fractions from SEC–HPLC were analyzed by dot blot decorated with anti-Hsp104 or anti-Aβ antibodies.

hydrolyzable ATP analogues or on the usage of the mutant Hsp104$_{TRAP}$.[4,36–38]

Discussion

ClpB/Hsp104 proteins have the ability to modulate aggregate formation and toxicity and to "catalyze" the disaggregation and recovery of protein aggregates in yeast,[12] *Escherichia coli*,[39] mammalian cell cultures, and animal models of HD and Parkinson's disease.[16–20] Several mechanistic models have been proposed to explain these experimental observations. These models include (i) Hsp104-mediated inhibition of protein misfolding and aggregation, (ii) diversion of proteins towards non-toxic pathways, and (iii) disruption and dissociation of prefibrillar and fibrillar toxic aggregates. To better understand the mechanisms by which Hsp104 modulates the aggregation of amyloid-forming proteins, the effect of Hsp104 on the different species along the amyloid fibril formation pathway of Aβ$_{42}$ was determined. Our findings show that Hsp104 inhibits the fibrillization of monomeric and protofibrillar forms of Aβ in a concentration-dependent but ATP-independent manner (Figs. 1–3). Strikingly, Hsp104 concentrations as low as 0.01 μM were sufficient to inhibit the fibrillization of 10 μM monomeric Aβ (Fig. 2). However, a highly efficient suppression of fibrillization was found at Hsp104 concentrations of 1 μM: no fibril formation was observed even after 10 days of incubation at 37 °C (Fig. 2).

Hsp104 inhibition of Aβ fibrillization is observable up to stoichiometric ratios of 1:1000 (Hsp104/Aβ, Fig. 2a-III), suggesting a preferential Hsp104 interaction with aggregation intermediates (e.g., oligomers, protofibrils, small fibrils) on the pathway of Aβ amyloid formation. This hypothesis is consistent with the current observations that Hsp104 (i) interacts with Aβ protofibrils (Figs. 3c-IIIb and 9b), (ii) inhibits conversion of protofibrils into amyloid fibrils (Fig. 3), (iii) arrests fibril elongation and reassembly (Fig. 6), and (iv) abolishes the capacity of protofibrils and SFs to seed the fibrillization of monomeric Aβ (Figs. 4 and 5). Together, these findings suggest that the strong inhibition of Aβ fibrillization by Hsp104 is mediated by its ability to act at different stages and target multiple intermediates on the pathway to amyloid formation

(Scheme 1c). Therefore, in addition to analyzing the effect of Hsp104 on the fibrillization of purified Aβ monomers, protofibrils, and fibrils, the ability of Hsp104 to arrest Aβ fibrillization at various stages along the fibrillization process, where a mixture of these different structures is present, was investigated. The addition of 1 μM Hsp104 at any time point during the fibrillization process resulted in complete inhibition and arrest of Aβ fibrillization as discerned by ThT and TEM data (Fig. 7). Even when Hsp104 was added during the exponential phase of Aβ fibrillization, a complete arrest of fibril formation was observed. Interestingly, in none of these samples a continuous decrease of ThT signal or an increase in soluble Aβ species (monomers, oligomers, protofibrils) was found, suggesting that Hsp104 inhibits fibrillization and blocks fibril elongation rather than mediates disaggregation of Aβ amyloids. However, one could speculate that a disaggregation activity only occurs if Hsp104 is assisted by other chaperones, such as Hsp70/Hsp40, which were not employed in this study.

In agreement with the current data reported here for Aβ$_{42}$, Inoue *et al.*[40] and Narayanan *et al.*[41] demonstrated that Hsp104 inhibits fibrillization of Sup35 fragments and Sup35NM in an ATP-independent manner. However, Hsp104 is thought to catalyze substrate unfolding by actively processing polypeptides through the central pore of its hexameric form with a substrate binding state that requires ATP or ATPγS.[4,5,7,36] Thus, the nucleotide-independent effect observed in the current work suggests a different type of substrate interaction of Hsp104 that results in an efficient inhibition of amyloid fibril formation.

In vitro studies by Shorter and colleagues[2,3] suggested that Hsp104 is a dual-function regulator of protein fibrillogenesis; i.e., it has the capacity to (i) catalyze amyloid formation and (ii) inhibit or disrupt preformed fibrils. The primary switch between the two opposing activities appeared to be the concentration of Hsp104. At low concentrations, Hsp104 was reported to catalyze the misfolding and fibrillization of amyloid-forming proteins such as the PrPs Sup35 and Ure2.[2,22] The authors proposed a general mechanism in which Hsp104 catalyzes fibrillization by fragmenting newly formed amyloid fibrils, thus increasing the number of fibrils ends and enhancing the seeding capacity of these proteins. A similar mechanism has been proposed to explain the role of Hsp104 in prion propagation of yeast cells, where Hsp104 fragments large insoluble prion aggregates into small prion seeds that are transmitted to daughter cells upon cell division.[13,42–45] This hypothesis is supported by the lack of polyQ aggregation in a yeast model of HD and by prion loss in yeast strains lacking Hsp104.[13,46] The *in vitro* data presented in the current study suggest that Hsp104 alone does not exhibit a dual concentration-dependent mechanism for modulating amyloid fibril formation; inhibition instead of acceleration of amyloid formation by Hsp104 was consistently observed. Interestingly, a

fusion protein of Sup35 and Aβ immediately aggregates in yeast cells and the resulting chimeric prion replicates independent of the presence of Hsp104.[47] These findings indicate that the mechanism of action by Hsp104 is highly dependent on the aggregation propensity of the substrate and differs among amyloid-forming proteins.

Taken together, the current study demonstrates a chaperoning activity of Hsp104 that contributes to the disaggregation activity reported by others and reveals a novel nucleotide-independent mechanism of fibril formation inhibition. Hsp104 was found to interact with different quaternary structures (monomer, protofibrils, and fibrils) along the fibrillization pathway of Aβ and inhibits their fibrillization (Scheme 1c). Furthermore, it was demonstrated that the inhibitory effect of Hsp104 is mediated by its inhibition of protofibrils and fibrils growth and self-assembly, rather than by Hsp104-induced disassembly of Aβ aggregates and fibrils. These mechanistic studies contribute significantly to our understanding of the molecular mechanism underlying ClpB/Hsp104 proteins and possibly other chaperones influencing amyloid formation and toxicity and have important implications for the prospects of using these molecules in future anti-aggregation-based therapeutic strategies.

Materials and Methods

Expression and purification of Hsp104

Hsp104$_{WT}$ and Hsp104$_{TRAP}$ were produced recombinantly in *E. coli* BL21 cells and purified as described.[34,48] Concentrations of Hsp104 were determined using an extinction coefficient of $\varepsilon_{276\,nm}=31{,}900\ \mathrm{M}^{-1}\,\mathrm{cm}^{-1}$ and refer to the monomeric species.

Monomeric and protofibrillar Aβ preparations

Aβ$_{42}$ peptide was synthesized and purified by Dr. James I. Elliott at Yale University (New Haven, CT) and purity was assessed by reverse-phase HPLC and mass spectrometry. To obtain monomeric Aβ, the peptide was dissolved in 6 M urea at 1 mg/ml followed by centrifugation in order to exclude insoluble material. The supernatant was loaded onto a Superdex 75 HR 10/30 SEC column (GE Healthcare) previously equilibrated with 10 mM Tris–HCl, pH 7.4, at a flow rate of 0.2 ml/min. To obtain both protofibrillar and monomeric fractions, a previously described protocol was followed.[49] Briefly, the peptide was dissolved in 100% dimethyl sulfoxide (DMSO) and adjusted to 1 mg/ml by adding double-distilled water followed by pH adjustment with 2 M Tris, pH 7.4, such that final concentrations of peptide, DMSO, and Tris were 200 μM, 5%, and 20 mM, respectively. After centrifugation, the supernatant was loaded onto a Superdex 75 HR 10/30 column. Peptide concentration was estimated by UV absorbance at 280 nm in 10-mm path-length cuvettes using the theoretical molar extinction coefficient at 280 nm (1490 M^{-1} cm^{-1}).[50] All given SF and protofibril concentrations refer to monomeric protein.

Fibrillization studies

Aβ samples, in the presence or absence of Hsp104, were incubated without agitation at 37 °C. The final concentrations of Aβ and Hsp104 were 10 and 1 μM, respectively, unless otherwise indicated. The final buffer composition was 25 mM Tris, pH 7.6, 37.5 mM KCl, 2.5 mM MgCl$_2$, 0.25% NaN$_3$. When indicated, samples contained, in addition, 5 mM ATP–Mg^{2+} or 1 mM ATPγS–Mg^{2+}. For the seeding experiments, first fibrils were generated by incubation of 10–20 μM monomeric Aβ at 37 °C for at least 96 h. The fibrils were then mechanically disrupted by ultrasonication with a fine tip. The SFs, or seeds, were added to the monomeric Aβ sample at a final concentration of 2.2 μM. Fibril formation and protein solubility was monitored by ThT fluorescence, negative-staining TEM, and SDS-PAGE as described below.

ThT binding assay

ThT binding assay was performed by mixing 10 μM peptide solution with 10 μM ThT dye (Aβ/ThT ratio = 1:1) and 50 mM glycine–NaOH, pH 8.5 (final concentrations) in Nunc384 well fluorescence plates (100 μl/well assay volume). ThT fluorescence of each sample was measured in an Analyst AD fluorometer (Molecular Devices) at excitation and emission wavelengths of 450 and 485 nm, respectively. The samples were analyzed in triplicates at selected time points and average fluorescence values and standard deviation were plotted.

Transmission electron microscopy

The samples (5–10 μl) were applied to carbon-coated formvar 200-mesh grids (Electron Microscopy Sciences, USA) and negatively stained with 2% uranyl acetate. EM grids were visualized in a Philips CM-10 TEM microscope at 100 kV and image acquisition was performed with a Morada TEM camera using iTEM 5 software (Olympus Soft Imaging Solutions).

SDS-PAGE analysis

To quantify the amount of Aβ remaining soluble in the samples, 50-μl aliqots were centrifuged at 13,200 rpm for 5 min and the supernatant was loaded onto 15% polyacrylamide gels under denaturing conditions. Silver staining (SilverXpress Silver Staining Kit, Invitrogen) was applied in order to detect the protein bands with a higher sensitivity.

ATPase assays

ATP hydrolysis by Hsp104 was monitored using a coupled enzymatic assay with an ATP-regenerating system consisting of PK and PEP as well as lactate dehydrogenase and NADH/H$^+$, as previously described.[34] Assays were performed at 30 °C in assay buffer (25 mM Tris, pH 7.6, 37.5 mM KCl, 8 mM MgCl$_2$, 0.25% NaN$_3$) containing 5 mM ATP and 0.2 μM Hsp104. Each ATPase experiment was started by monitoring the absorbance of NADH at 340 nm including all assay components except Hsp104. When the signal was settled as a flat line, the reaction was started by the addition of Hsp104. The ATP turnover of Hsp104 was determined from the slope d$A_{340\ nm}$/dt using a molar absorbance coefficient for NADH of $\varepsilon_{340\ nm} = 6200\ M^{-1}\ cm^{-1}$ as described.[5] For each data point, three independent measurements were carried out to calculate the mean and the standard deviation for each sample set.

SEC–HPLC co-elution experiments

Samples containing 5 μM Hsp104$_{WT}$, with or without 40 μM Aβ monomer, or 100 μM Aβ protofibrils were prepared in 25 mM Tris, pH 7.6, 37.5 mM KCl, and 2.5 mM MgCl$_2$ and incubated at 25 °C for 30 min. A sample of 35 μl was separated at a flow rate of 0.08 ml/min on a Superose 6 PC3.2/30 column (GE Healthcare) equilibrated with the sample buffer described above. The absorbance of the proteins was monitored at 214 nm and fractions were collected every minute. For dot blot analysis, 1.8 μl of each fraction was placed on a membrane and visualized using anti-Hsp104 antibodies (rabbit) or anti-Aβ antibodies (mouse).

Supplementary Data

Supplementary data associated with this article can be found, in the online version, at doi:10.1016/j.jmb.2008.09.063

References

1. Lansbury, P. T. & Lashuel, H. A. (2006). A century-old debate on protein aggregation and neurodegeneration enters the clinic. *Nature*, **443**, 774–779.
2. Shorter, J. & Lindquist, S. (2004). Hsp104 catalyzes formation and elimination of self-replicating Sup35 prion conformers. *Science*, **304**, 1793–1797.
3. Shorter, J. & Lindquist, S. (2006). Destruction or potentiation of different prions catalyzed by similar Hsp104 remodeling activities. *Mol. Cell*, **23**, 425–438.
4. Bösl, B., Grimminger, V. & Walter, S. (2005). Substrate binding to the molecular chaperone Hsp104 and its regulation by nucleotides. *J. Biol. Chem.* **280**, 38170–38176.
5. Schaupp, A., Marcinowski, M., Grimminger, V., Bösl, B. & Walter, S. (2007). Processing of proteins by the molecular chaperone Hsp104. *J. Mol. Biol.* **370**, 674–686.

6. Bösl, B., Grimminger, V. & Walter, S. (2006). The molecular chaperone Hsp104-A molecular machine for protein disaggregation. *J. Struct. Biol.* **156**, 139–148.

7. Doyle, S. M., Shorter, J., Zolkiewski, M., Hoskins, J. R., Lindquist, S. & Wickner, S. (2007). Asymmetric deceleration of ClpB or Hsp104 ATPase activity unleashes protein-remodeling activity. *Nat. Struct. Mol. Biol.* **14**, 114–122.

8. Wendler, P., Shorter, J., Plisson, C., Cashikar, A. G., Lindquist, S. & Saibil, H. R. (2007). Atypical AAA+ subunit packing creates an expanded cavity for disaggregation by the protein-remodeling factor Hsp104. *Cell*, **131**, 1366–1377.

9. Weibezahn, J., Tessarz, P., Schlieker, C., Zahn, R., Maglica, Z., Lee, S. *et al.* (2004). Thermotolerance requires refolding of aggregated proteins by substrate translocation through the central pore of ClpB. *Cell*, **119**, 653–665.

10. Zolkiewski, M. (2006). A camel passes through the eye of a needle: protein unfolding activity of Clp ATPases. *Mol. Microbiol.* **61**, 1094–1100.

11. Ben Zvi, A. P. & Goloubinoff, P. (2001). Mechanisms of disaggregation and refolding of stable protein aggregates by molecular chaperones. *J. Struct. Biol.* **135**, 84–93.

12. Glover, J. R. & Lindquist, S. (1998). Hsp104, Hsp70, and Hsp40: a novel chaperone system that rescues previously aggregated proteins. *Cell*, **94**, 73–82.

13. Chernoff, Y. O., Lindquist, S. L., Ono, B., Inge-Vechtomov, S. G. & Liebman, S. W. (1995). Role of the chaperone protein Hsp104 in propagation of the yeast prion-like factor [psi+]. *Science*, **268**, 880–884.

14. Sanchez, Y. & Lindquist, S. L. (1990). HSP104 required for induced thermotolerance. *Science*, **248**, 1112–1115.

15. Sanchez, Y., Taulien, J., Borkovich, K. A. & Lindquist, S. (1992). Hsp104 is required for tolerance to many forms of stress. *EMBO J.* **11**, 2357–2364.

16. Carmichael, J., Chatellier, J., Woolfson, A., Milstein, C., Fersht, A. R. & Rubinsztein, D. C. (2000). Bacterial and yeast chaperones reduce both aggregate formation and cell death in mammalian cell models of Huntington's disease. *Proc. Natl Acad. Sci. USA*, **97**, 9701–9705.

17. Cashikar, A. G., Duennwald, M. & Lindquist, S. L. (2005). A chaperone pathway in protein disaggregation. Hsp26 alters the nature of protein aggregates to facilitate reactivation by Hsp104. *J. Biol. Chem.* **280**, 23869–23875.

18. Perrin, V., Regulier, E., Abbas-Terki, T., Hassig, R., Brouillet, E., Aebischer, P. *et al.* (2007). Neuroprotection by Hsp104 and Hsp27 in lentiviral-based rat models of Huntington's disease. *Mol. Ther.* **15**, 903–911.

19. Satyal, S. H., Schmidt, E., Kitagawa, K., Sondheimer, N., Lindquist, S., Kramer, J. M. & Morimoto, R. I. (2000). Polyglutamine aggregates alter protein folding homeostasis in *Caenorhabditis elegans*. *Proc. Natl Acad. Sci. USA*, **97**, 5750–5755.

20. Vacher, C., Garcia-Oroz, L. & Rubinsztein, D. C. (2005). Overexpression of yeast hsp104 reduces polyglutamine aggregation and prolongs survival of a transgenic mouse model of Huntington's disease. *Hum. Mol. Genet.* **14**, 3425–3433.

21. Kimura, Y., Koitabashi, S., Kakizuka, A. & Fujita, T. (2001). Initial process of polyglutamine aggregate formation in vivo. *Genes Cells*, **6**, 887–897.

22. DebBurman, S., Raymond, G., Caughey, B. & Lindquist, S. (1997). Chaperone-supervised conversion of prion protein to its protease-resistant form. *Proc. Natl. Acad. Sci. USA*, **94**, 13938–13943.

23. Schirmer, E. C. & Lindquist, S. L. (1997). Interactions of the chaperone Hsp104 with yeast Sup35 and mammalian PrP. *Proc. Natl Acad. Sci. USA*, **94**, 13932–13937.

24. Lashuel, H. A. & Grillo-Bosch, D. (2005). In vitro preparation of prefibrillar intermediates of amyloid-beta and alpha-synuclein. *Methods Mol. Biol.* **299**, 19–33.

25. Jan, A., Gokce, O., Luthi-Carter, R. & Lashuel, H. A. (2008). The ratio of monomeric to aggregated forms of Abeta40 and Abeta42 is an important determinant of Aabeta aggregation, fibrillogenesis, and toxicity. *J. Biol. Chem.* **283**, 28176–28189.

26. Harper, J. D., Lieber, C. M. & Lansbury, P. T., Jr. (1997). Atomic force microscopic imaging of seeded fibril formation and fibril branching by the Alzheimer's disease amyloid-beta protein. *Chem. Biol.* **4**, 951–959.

27. Harper, J. D., Wong, S. S., Lieber, C. M. & Lansbury, P. T. (1997). Observation of metastable Abeta amyloid protofibrils by atomic force microscopy. *Chem. Biol.* **4**, 119–125.

28. Walsh, D. M., Lomakin, A., Benedek, G. B., Condron, M. M. & Teplow, D. B. (1997). Amyloid beta-protein fibrillogenesis. Detection of a protofibrillar intermediate. *J. Biol. Chem.* **272**, 22364–22372.

29. Arimon, M., Diez-Perez, I., Kogan, M. J., Durany, N., Giralt, E., Sanz, F. & Fernandez-Busquets, X. (2005). Fine structure study of Abeta1–42 fibrillogenesis with atomic force microscopy. *FASEB J.* **19**, 1344–1346.

30. Bitan, G., Kirkitadze, M. D., Lomakin, A., Vollers, S. S., Benedek, G. B. & Teplow, D. B. (2003). Amyloid beta-protein (Abeta) assembly: Abeta 40 and Abeta 42 oligomerize through distinct pathways. *Proc. Natl Acad. Sci. USA*, **100**, 330–335.

31. Harper, J. D., Wong, S. S., Lieber, C. M. & Lansbury, P. T., Jr. (1999). Assembly of A beta amyloid protofibrils: an in vitro model for a possible early event in Alzheimer's disease. *Biochemistry*, **38**, 8972–8980.

32. Harper, J. D. & Lansbury, P. T., Jr (1997). Models of amyloid seeding in Alzheimer's disease and scrapie: mechanistic truths and physiological consequences of the time-dependent solubility of amyloid proteins. *Annu. Rev. Biochem.* **66**, 385–407.

33. Jarrett, J. T. & Lansbury, P. T., Jr (1993). Seeding "one-dimensional crystallization" of amyloid: a pathogenic mechanism in Alzheimer's disease and scrapie? *Cell*, **73**, 1055–1058.

34. Grimminger, V., Richter, K., Imhof, A., Buchner, J. & Walter, S. (2004). The prion curing agent guanidinium chloride specifically inhibits ATP hydrolysis by Hsp104. *J. Biol. Chem.* **279**, 7378–7383.

35. Cashikar, A. G., Schirmer, E. C., Hattendorf, D. A., Glover, J. R., Ramakrishnan, M. S., Ware, D. M. & Lindquist, S. L. (2002). Defining a pathway of communication from the C-terminal peptide binding domain to the N-terminal ATPase domain in a AAA protein. *Mol. Cell*, **9**, 751–760.

36. Weibezahn, J., Schlieker, C., Bukau, B. & Mogk, A. (2003). Characterization of a trap mutant of the AAA+ chaperone ClpB. *J. Biol. Chem.* **278**, 32608–32617.

37. Barnett, M. E., Nagy, M., Kedzierska, S. & Zolkiewski, M. (2005). The amino-terminal domain of ClpB supports binding to strongly aggregated proteins. *J. Biol. Chem.* **280**, 34940–34945.

38. Schlieker, C., Weibezahn, J., Patzelt, H., Tessarz, P., Strub, C., Zeth, K. *et al.* (2004). Substrate recognition by the AAA+ chaperone ClpB. *Nat. Struct. Mol. Biol.* **11**, 607–615.

39. Goloubinoff, P., Mogk, A., Zvi, A. P., Tomoyasu, T. & Bukau, B. (1999). Sequential mechanism of solubilization and refolding of stable protein aggregates by a bichaperone network. *Proc. Natl Acad. Sci. USA*, **96**, 13732–13737.

40. Inoue, Y., Taguchi, H., Kishimoto, A. & Yoshida, M. (2004). Hsp104 binds to yeast Sup35 prion fiber but needs other factor(s) to sever it. *J. Biol. Chem.* **279**, 52319–52323.

41. Narayanan, S., Bösl, B., Walter, S. & Reif, B. (2003). Importance of low-oligomeric-weight species for prion propagation in the yeast prion system Sup35/ Hsp104. *Proc. Natl Acad. Sci. USA*, **100**, 9286–9291.

42. Kushnirov, V. V. & Ter Avanesyan, M. D. (1998). Structure and replication of yeast prions. *Cell*, **94**, 13–16.

43. Ness, F., Ferreira, P., Cox, B. S. & Tuite, M. F. (2002). Guanidine hydrochloride inhibits the generation of prion "seeds" but not prion protein aggregation in yeast. *Mol. Cell Biol.* **22**, 5593–5605.

44. Paushkin, S. V., Kushnirov, V. V., Smirnov, V. N. & Ter Avanesyan, M. D. (1996). Propagation of the yeast prion-like [psi+] determinant is mediated by oligomerization of the SUP35-encoded polypeptide chain release factor. *EMBO J.* **15**, 3127–3134.

45. Satpute-Krishnan, P., Langseth, S. X. & Serio, T. R. (2007). Hsp104-dependent remodeling of prion complexes mediates protein-only inheritance. *PLoS Biol.* **5**, e24.

46. Krobitsch, S. & Lindquist, S. (2000). Aggregation of huntingtin in yeast varies with the length of the polyglutamine expansion and the expression of chaperone proteins. *Proc. Natl Acad. Sci. USA*, **97**, 1589–1594.

47. von der Haar, T., Josse, L., Wright, P., Zenthon, J. & Tuite, M. F. (2007). Development of a novel yeast cell-based system for studying the aggregation of Alzheimer's disease-associated Abeta peptides in vivo. *Neurodegener. Dis.* **4**, 136–147.

48. Schirmer, E. C. & Lindquist, S. (1998). Purification and properties of Hsp104 from yeast. *Methods Enzymol.* **290**, 430–444.

49. Lashuel, H. A., Hartley, D. M., Petre, B. M., Wall, J. S., Simon, M. N., Walz, T. & Lansbury, P. T., Jr (2003). Mixtures of wild-type and a pathogenic (E22G) form of Abeta40 in vitro accumulate protofibrils, including amyloid pores. *J. Mol. Biol.* **332**, 795–808.

50. Pace, C. N., Vajdos, F., Fee, L., Grimsley, G. & Gray, T. (1995). How to measure and predict the molar absorption coefficient of a protein. *Protein Sci.* **4**, 2411–2423.